Biomaterials 34 (2013) 9566–9571

Contents lists available at ScienceDirect

Biomaterials

journal homepage: www.elsevier.com/locate/biomaterials

Analogs of Changsha near-infrared dyes with large Stokes Shifts for bioimaging

Lin Yuan, Weiying Lin*, Hua Chen

State Key Laboratory of Chemo/Biosensing and Chemometrics, College of Chemistry and Chemical Engineering, Hunan University, Changsha, Hunan 410082, PR China

ARTICLE INFO

Article history:
Received 8 July 2013
Accepted 27 August 2013
Available online 17 September 2013

Keywords:
Fluorescent probes
Near-infrared dyes
Stokes shifts
Hypochlorous acid
Bioimaging

ABSTRACT

The construction of fluorescent imaging probes has contributed significantly to the recent advances in biology and medicine. Near infrared (NIR) fluorescent probes are favorable to be employed in fluorescence imaging in living animals. Rhodamine dyes have been widely used as a robust platform for development of fluorescent probes for a wide variety of targets. However, the absorption and emission wavelengths of classical rhodamine derivatives are below 600 nm. Thus, it is desirable to construct rhodamine analogs with longer absorption and emission wavelengths, preferably in the NIR region. Toward this end, our group has previously constructed Changsha (CS) NIR dyes while retaining the rhodamine-like fluorescence ON–OFF switching mechanism. However, like classic rhodamines, these rhodamine NIR derivatives still have small Stokes shifts (typically less than 35 nm), which can lead to serious self-quenching and fluorescence detection error due to excitation backscattering effects. This shortcoming may constrain the full potential of their applications. Thus, there is a need to develop rhodamine NIR derivatives with large Stokes shifts. In this work, we have designed and synthesized a class of analogs of CS NIR dyes with large Stokes shifts. Among the new dyes presented herein, the dye **1c** displays a high fluorescence quantum yield in biological media and thus promising for *in vivo* imaging applications. Furthermore, using **1c** as a platform, we further constructed the NIR fluorescent turn-on probe **3**, which is suitable for imaging endogenously produced HClO in the RAW264.7 macrophage cells, demonstrating the value of our new NIR functional fluorescent dye **1c**.

1. Introduction

Fluorescence imaging has emerged as a very powerful technique for monitoring biomolecules of interest in living systems [1–6]. The development of effective fluorescent imaging probes has facilitated the recent significant advances in cell biology and medical diagnostics [4–18]. When compared to fluorescent probes with emission in the visible light region, near infrared (NIR) fluorescent probes are advantageous to be employed in biological imaging as NIR light (650–900 nm) leads to minimum photo-damage to biological samples, deep tissue penetration due to very little undesired absorption by biomolecules and diminishing Rayleigh–Tyndall scattering of light, and minimum interference from background auto-fluorescence by biomolecules in the living systems [19,20].

Among the various organic fluorophores, the rhodamine dyes have received great attention due to their excellent photophysical properties, high molar extinction coefficients, large fluorescence quantum yields, and tolerance to photobleaching [21,22]. In addition, importantly, the fluorescence of rhodamines can be controlled by the unique spirolactam ring-opening and -closing process. These favorable attributes render rhodamines a robust platform for development of fluorescent probes for a wide variety of targets [21,22]. However, the absorption and emission wavelengths of classical rhodamine derivatives are below 600 nm. Thus, it is desirable to construct rhodamine analogs with longer absorption and emission wavelengths, preferably in the NIR region. Toward this end, Nagano's group has developed Si-rhodamines [23] and our group has constructed Changsha (CS) NIR dyes [24] while retaining the rhodamine-like fluorescence ON–OFF switching mechanism.

However, like classic rhodamines, these rhodamine NIR derivatives still have small Stokes shifts (typically less than 35 nm), which can lead to serious self-quenching and fluorescence detection error due to excitation backscattering effects [25]. This shortcoming may constrain the full potential of their applications. Thus, there is a need to develop rhodamine NIR derivatives with large Stokes shifts.

* Corresponding author. Fax: +86 731 88821464.
E-mail addresses: weiyinglin@hnu.edu.cn, weiyinglin2013@163.com (W. Lin).

0142-9612/$ – see front matter © 2013 Elsevier Ltd. All rights reserved.
http://dx.doi.org/10.1016/j.biomaterials.2013.08.081

HOCl, one of the biologically significant ROS, is produced from peroxidation of chloride ions catalyzed by the enzyme myeloperoxidase (MPO) in activated leukocytes [26]. However, abnormal levels of HOCl are implicated with various diseases such as cardiovascular diseases, rheumatoid arthritis, and cancer [27]. Thus, the detection of endogenously produced HClO in living systems is of high interest [23,28–30].

Herein, we describe the development of a new class of dyes represented by **1a**–**f** as the first paradigm of rhodamine long wavelength analogs with large Stokes shifts (Fig. 1). To demonstrate that the new type of dyes, like classic rhodamines, can be used as a platform to design fluorescent probes for bioimaging applications, we further engineered a new HOCl probe based on the dye **1c**.

2. Materials and methods

2.1. Materials and instruments

Compounds **4a**–**d** are commercially available and compounds **5** [24], **4e** [31], and **4f** [32] were synthesized in our previous work. Unless otherwise stated, all reagents were purchased from commercial suppliers and used without further purification. Solvents used were purified by standard methods prior to use. Twice-distilled water was used throughout all experiments. Low resolution mass spectra were performed using an LCQ Advantage ion trap mass spectrometer from Thermo Finnigan or Agilent 1100 HPLC/MSD spectrometer; high-resolution electronspray (ESI-HRMS) mass spectra were obtained from Bruker APEX IV-FTMS 7.0 T mass spectrometer; NMR spectra were recorded on an INOVA-400 spectrometer, using TMS as an internal standard; Electronic absorption spectra were obtained on a LabTech UV Power spectrometer; Photoluminescent spectra were recorded with a HITACHI F4600 fluorescence spectrophotometer; Cells imaging was performed with a Olympus fluorescence microscopy equipped with a cooled CCD camera; The pH measurements were carried out on a Mettler-Toledo Delta 320 pH meter; TLC analysis was performed on silica gel plates and column chromatography was conducted over silica gel (mesh 200–300), both of which were obtained from the Qingdao Ocean Chemicals.

2.2. Determination of the fluorescence quantum yield

Fluorescence quantum yields for **1a**–**f** were determined by using ICG ($\Phi_f = 0.13$ in DMSO) as a fluorescence standard [33]. The quantum yield was calculated using the following equation:

$$\Phi_{F(X)} = \Phi_{F(S)}(A_S F_X / A_X F_S)(n_X / n_S)^2$$

where Φ_F is the fluorescence quantum yield, A is the absorbance at the excitation wavelength, F is the area under the corrected emission curve, and n is the refractive index of the solvents used. Subscripts S and X refer to the standard and to the unknown, respectively.

2.3. Raw 264.7 murine macrophages culture and imaging using probe **3**

Raw 264.7 murine macrophages were obtained from the third Xiangya hospital and cultured in DMEM (Dulbecco's Modified Eagle Medium) supplemented with 10% FBS (fetal bovine serum) in an atmosphere of 5% CO_2 and 95% air at 37 °C. For detection of endogenously produced HOCl, the living RAW 264.7 macrophages were treated with LPS (1 μg/mL) for 12 h, and then further co-incubated with PMA (1 μg/mL), and probe **3** (5 μM) for 60 min. Prior to imaging, the cells were washed three times with 1 mL of PBS and the fluorescence images were acquired through an Olympus fluorescence microscopy equipped with a cooled CCD camera.

2.4. Fluorescence imaging in living mice using dye **1c**

20–25 g ICR mice were anesthetized by an i.p. injection of xylazine (10 mg/kg) and ketamine (80 mg/kg) and the abdominal fur was removed with an electric shave. Then, the mice were given an intraperitoneal (i.p.) injection of dye **1c** (400 μM in 400 μL of PBS, containing 5% CH_3OH). The mice were imaged (10 min after the injection of dye **1c**) by using an FMT 2500 LX Quantitative Tomography In Vivo Imaging System, with an excitation filter of 670 nm and an emission filter of 690–740 nm.

2.5. Cytotoxicity assays

Raw 264.7 murine macrophages were cultured in DMEM (Dulbecco's Modified Eagle Medium) supplemented with 10% FBS supplemented with 100 U/mL of penicillin and 100 μg/mL streptomycin in an atmosphere of 5% CO_2 and 95% air at 37 °C. The cells were seeded into 96-well plates, and then 1, 2.5, 5.0, 7.5, 10.0, or 15.0 μM (final concentration) probe **3** (99.9% DMEM and 0.1% DMSO) was added respectively ($n = 6$). Subsequently, the cells were incubated at 37 °C in an atmosphere of 5% CO_2 and 95% air for 12 h. Untreated assay with DMEM ($n = 6$) was also conducted under the same conditions.

2.6. Synthesis of compounds ***1a–f***

Compound **5** (0.21 mmol) and substituted benzaldehyde **4a**–**f** (0.25 mmol) were dissolved in acetic acid (4 ml), and the reaction mixture was heated to 90–100 °C for 2–5 h. Then, the solvent was removed under reduced pressure to give the crude product, which was purified by silica gel flash chromatography using from CH_2Cl_2 to CH_2Cl_2/ethanol (200:1 to 10:1) as eluant to afford compounds **1a** (yield 80%) and **1b** (yield 95%) as purple solid, **1c** (yield 90%) and **1d** (yield 70%) as blue solid, and **1e** (yield >90%) and **1f** (yield 70%) as green solid.

2.6.1. Compound ***1a***

^{1}H NMR (DMSO, 400 MHz) δ 1.09 (t, $J = 7.2$ Hz, 6H), 1.55–1.60 (3H), 1.83–1.86 (1H), 2.61 (1H), 2.73–2.77 (1H), 3.33–3.36 (q, 4H), 6.40 (d, $J = 8.4$ Hz, 1H), 6.47 (d, $J = 7.2$ Hz, 1H), 6.55 (s, 1H), 6.82 (d, $J = 8.8$ Hz, 2H), 7.29–7.34 (4H), 7.67 (t, $J = 7.4$ Hz, 1H), 7.79 (t, $J = 7.6$ Hz, 1H), 7.95 (d, $J = 7.6$ Hz, 1H), 9.70 (s, 1H, OH); ^{13}C NMR (DMSO, 100 MHz) δ 12.7, 22.2, 23.0, 26.9, 44.1, 96.9, 97.1, 104.9, 107.4, 109.5, 115.5, 124.1, 125.1, 125.9, 127.2, 127.5, 127.5, 128.6, 130.2, 131.4, 135.5, 147.5, 149.5, 152.3, 157.2, 169.3; MS (ESI) m/z 480.2 $(M - ClO_4^-)^+$; HRMS (ESI) m/z calcd for $C_{36}H_{37}N_2O_3^+$ $C_{36}H_{37}N_2O_3^+$ $(M - ClO_4^-)^+$: 480.2175. Found 480.2148.

2.6.2. Compound ***1b***

^{1}H NMR (DMSO, 400 MHz) δ 1.09 (t, $J = 6.8$ Hz, 6H), 1.54–1.57 (3H), 1.82–1.84 (1H), 2.58–2.60 (1H), 2.75–2.78 (1H), 3.33–3.36 (q, 4H), 6.39 (d, $J = 9.2$ Hz, 1H), 6.45- (d, $J = 9.2$ Hz, 1H), 6.55 (s, 1H), 7.02 (d, $J = 8.4$ Hz, 1H), 7.27 (d, $J = 9.6$ Hz, 1H), 7.31 (d, $J = 7.2$ Hz, 2H), 7.44 (s, 1H), 7.67 (t, $J = 7.6$ Hz, 1H), 7.79 (t, $J = 7.6$ Hz, 1H), 7.95 (d, $J = 8.0$ Hz, 1H), 10.45 (s, 1H, OH); ^{13}C NMR (DMSO, 100 MHz) δ 12.7, 22.2, 22.9, 26.9, 44.0, 96.9, 97.1, 109.4, 116.7, 119.9, 124.0, 124.4, 125.1, 127.1, 128.5, 128.8, 128.9, 129.7, 130.2, 131.2, 135.5, 149.4, 152.1, 152.7, 169.3; MS (ESI) m/z 514.3 $(M - ClO_4^-)^+$; HRMS (ESI) m/z calcd for $C_{36}H_{37}N_2O_3^+$ $(M - ClO_4^-)^+$: 514.1785. Found 514.1788.

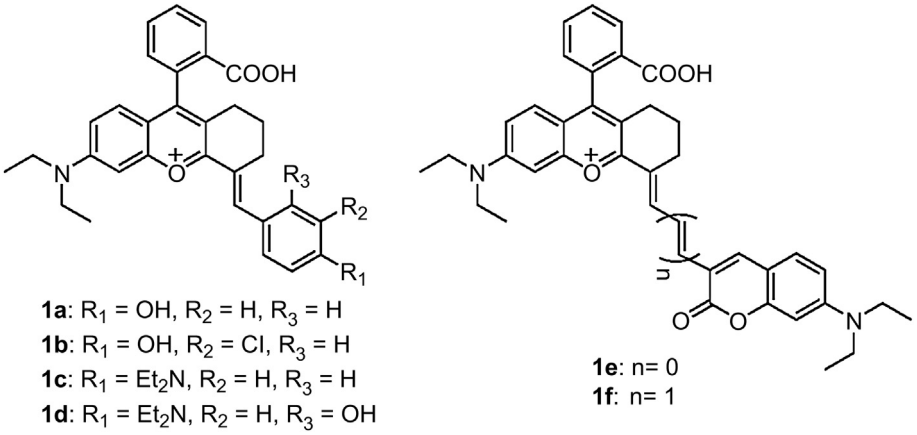

Fig. 1. The structures of dyes **1a**–**f**.